

Over 3 W high-efficiency vertical-external-cavity surface-emitting lasers and application as efficient fiber laser pump sources

L. Fan^{a)} and M. Fallahi

Optical Sciences Center, University of Arizona, Tucson, Arizona 85721

J. Hader, A. R. Zakharian, M. Kolesik, and J. V. Moloney

Arizona Center for Mathematical Science, University of Arizona, Tucson, Arizona 85721

T. Qiu, A. Schülzgen, and N. Peyghambarian

Optical Sciences Center, University of Arizona, Tucson, Arizona 85721

W. Stolz and S. W. Koch

Material Sciences Center and Department of Physics, Philipps Universität Marburg, Renthof 5, 35032 Marburg, Germany

J. T. Murray

Areté Associates, 333 N. Wilmot Road, Ste 450, Tucson, Arizona 85751-2348

(Received 25 October 2004; accepted 13 April 2005; published online 18 May 2005)

We report on the design and fabrication of high-power, high-brightness diode-pumped vertical-external-cavity surface-emitting lasers. Over 3 W continuous wave fundamental transverse mode (TEM_{00}) output at 980 nm with a high slope efficiency of 44% is demonstrated at room temperature. The diffraction-limited beam with M^2 factor of 1.15 at high-power operation is achieved. A vertical-external-cavity surface-emitting laser operating near 976 nm with a diffraction-limited beam is used to pump the core of 3 cm long Er/Yb-codoped single-mode phosphate fiber lasers. An output power in excess of 250 mW at 1535 nm with a slope efficiency of 29% is obtained without any cooling. © 2005 American Institute of Physics.

[DOI: 10.1063/1.1935756]

High-power high-brightness lasers are the key elements for a wide range of commercial and defense applications. Optically pumped semiconductor vertical-external-cavity surface-emitting lasers (VECSELs) are particularly attractive for their high power and excellent beam quality.¹⁻⁴ They can be used in a wide range of applications, including fiber laser pump source, intracavity frequency doubling, lidar, and free space communication. VECSELs combine the techniques of diode-pumped solid-state thin disk lasers and semiconductor quantum-well vertical-cavity surface-emitting lasers. In these lasers, a semiconductor multiquantum wells' (MQW) active region and a distributed Bragg reflector (DBR) stack, only a few microns thick, is mounted on the heat spreader or heat sink, resulting in efficient heat dissipation which makes VECSEL a strong candidate in power-scalable lasers.⁵ Optical pumping of multiquantum wells is the most straightforward way to achieve a uniform carrier distribution over a large pump area, and is particularly advantageous for multi-watt operation. The external output coupler (mirror) controls the transverse mode operation. Other reports of similar VECSELs have been published where output power has been scaled up to 8–10 W with high beam quality, using a larger pump spot than was used in this work.^{2,3}

In this letter, we report on the development of a high-power high-brightness VECSEL with TEM_{00} transverse mode and its use as an efficient pump source for single-mode fiber lasers. Over 3 W continuous-wave (cw) TEM_{00} ($M^2 = 1.15$) output and a high slope efficiency of 44% are achieved at room temperature for 220 μm diameter pump

spot. A VECSEL operating at 976 nm is used to pump the core of a 3 cm long highly doped erbium/ytterbium (Er/Yb) single-mode phosphate fiber laser. An output in excess of 250 mW with high slope of 29% is achieved at 1535 nm without any cooling.

High-power cw operation of VECSEL requires high-gain MQW structures combined with efficient heat extraction from the active region. Based on the microscopic many-body theory,⁶ the VECSEL structure is designed for emission around 980 nm. To delay the thermal rollover, the active region is designed so that the quantum-well gain peak is blueshifted initially with respect to the microcavity resonance,⁷ to account for a higher rate of thermally induced shift of the gain peak, compared to the rate of shift of the microcavity resonance. The VECSEL structure was grown by metalorganic vapor phase epitaxy (MOVPE) on an undoped GaAs substrate. The active region consists of 14 InGaAs compressive strained quantum wells. Each quantum well is 8 nm thick and surrounded by GaAsP strain compensation layers and AlGaAs absorbing barriers. The thickness and compositions of the layers are optimized such that each quantum well is positioned at an antinode of the standing wave of the laser field to provide resonant periodic gain (RPG) in the active region. Figure 1 shows the schematic cross section of the structure. A high reflectivity ($R > 99.9\%$) DBR stack made of 25 pairs of AlGaAs/AlAs is grown on the top of the active region. In addition to the RPG active region and DBR stack, there is a high aluminum concentration AlGaAs etch-stop layer between the active region and the substrate to facilitate selective chemical substrate removal.

^{a)}Electronic mail: lifan@optics.arizona.edu

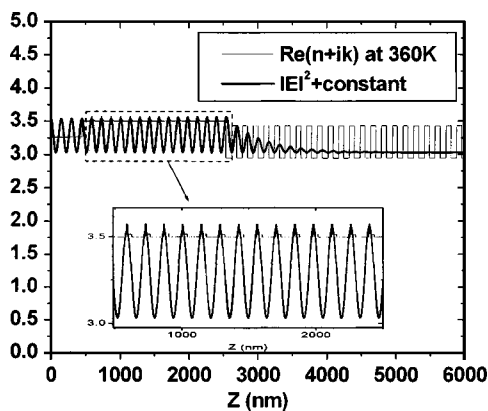


FIG. 1. Refractive index profile through the VECSEL structure with the standing wave pattern for the lasing wavelength at 975 nm.

The fabrication of the VECSEL is critical to the laser performance. The VECSEL should have high surface quality to minimize scattering/diffraction losses and efficient heat extraction from the active region to avoid thermal rollover and thermal lensing. To achieve this goal, a high thermal conductivity ($>15 \text{ W cm}^{-1} \text{ K}^{-1}$) chemical vapor deposition (CVD) diamond with high surface quality (peak-to-valley height $<100 \text{ nm}$) is used as the submount/heat spreader. The fabrication process includes sample mounting and substrate removal. First, the epitaxial side of a $2 \text{ mm} \times 2 \text{ mm}$ VECSEL wafer and CVD diamond are metallized with titanium and gold. Then, the wafer is mounted on CVD diamond by soft indium solder, which has high thermal conductivity and can reduce thermal stress at the semiconductor/submount interface. Since the lasing wavelength of the VECSEL and resonance of microcavity strongly depend on the semiconductor microcavity thickness,¹ the substrate and etch-stop removal must be well controlled to obtain the proper semiconductor microcavity thickness and the optically smooth surface. The substrate is first etched to a thickness of about $50 \mu\text{m}$ by a fast nonselective wet chemical etching using $\text{H}_2\text{SO}_4:\text{H}_2\text{O}:\text{H}_2\text{O}_2$. The remaining GaAs substrate is subsequently removed by selective wet chemical etching using $\text{C}_6\text{H}_8\text{O}_7:\text{H}_2\text{O}_2$. After the substrate removal, a diluted hydrofluoric acid is used to remove the AlGaAs etch-stop layer. After substrate removal, the remaining semiconductor is only $6.5 \mu\text{m}$ thick, allowing efficient heat dissipation at high pumping energy. The surface quality of the VECSEL sample is then characterized by the interferometer, WYKO NT-2000, and a peak-to-valley height of less than 50 nm in an area of $0.5 \text{ mm} \times 0.5 \text{ mm}$ can be achieved. This optically smooth surface makes the scattering/diffraction loss negligible and results in high slope efficiency and high beam quality.

The processed sample is mounted on a thermoelectric cooler for temperature control. The lasing experiment is conducted by using a fiber coupled multimode 808 nm diode laser pump source. The pump light from the fiber, with $100 \mu\text{m}$ core fiber diameter and 0.22 numerical aperture, is focused onto the sample by a relay lens with 18 mm focal length at an incident angle of 30° . The pump spot size, as determined by photoluminescence emission, is adjusted to be $220 \mu\text{m}$ in diameter. As the sample is uncoated, about 27% incident pump power is reflected at the semiconductor/air interface. This amount can be reduced by a lower reflectivity coating on the surface of the processed semiconductor. The external cavity is formed using a concave mirror with 10 cm

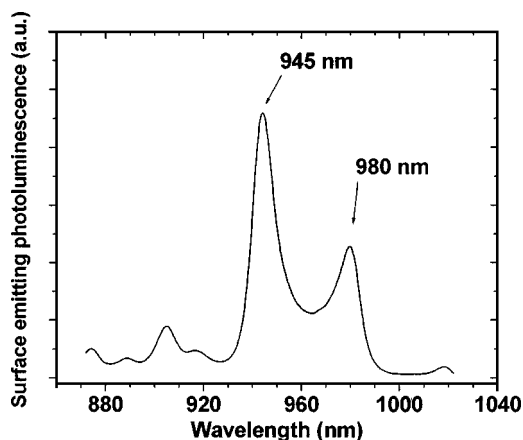


FIG. 2. Surface-emitting PL spectrum from the VECSEL sample.

radius of curvature and 96% reflectivity. The cavity length was adjusted for maximum TEM_{00} output.

Before building the external cavity, the surface-emitting photoluminescence (PL) spectrum is captured normally to the sample surface by a multimode fiber. The surface-emitting PL spectrum is a convolution of the quantum-well PL, DBR reflector, and the microcavity formed by the DBR and semiconductor/air interface etalon. It can be used as a tool to measure the characteristic of spontaneous emission inside the microcavity, and to estimate the material gain peak wavelength. Figure 2 shows the surface-emitting PL spectrum at a low pump level. There are two major peaks around 946 nm and 980 nm. They correspond to the longitudinal resonance modes in the microcavity that fit the DBR bandwidth. The peak around 945 nm is stronger than the peak around 980 nm at lower pump level, suggesting that the quantum-well gain peak wavelength is blueshifted with respect to the lasing wavelength (around 980 nm). This is an agreement with the design and allows the VECSEL to operate with high pump power before the thermal rollover.

The VECSEL is characterized at room temperature ($\sim 20^\circ \text{C}$). Figure 3 shows the TEM_{00} output power as a function of net pump power. For a $220 \mu\text{m}$ diameter pump spot, a cw TEM_{00} output power of 3.1 W with a slope efficiency (SE) of 44% is achieved. To characterize the spatial (transverse) mode of the VECSEL, the output beam is focused by an objective lens into a real-time beam profiler Beam-MAP (DataRay Inc.) to measure the value of the M^2 factor as the criteria of VECSEL beam quality. Measured values of M^2

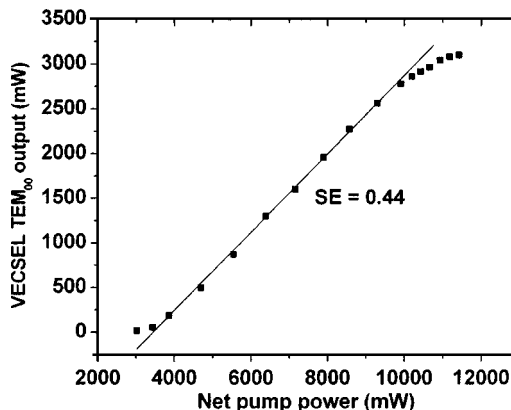


FIG. 3. VECSEL TEM_{00} cw output power at 980 nm vs net pump power at room temperature ($\sim 20^\circ \text{C}$).

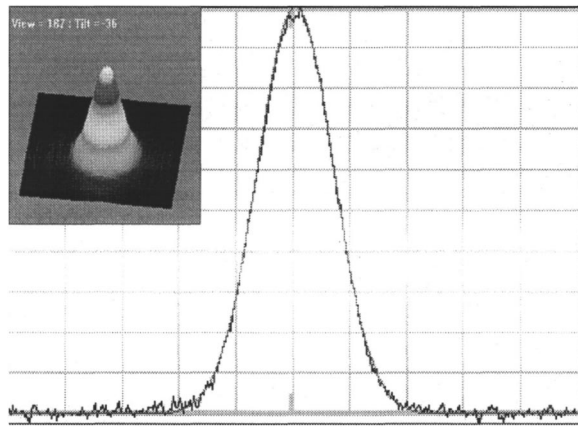


FIG. 4. 3D VECSEL beam profile and Gaussian fit along the cross section of the beam at high-power operation.

factor are 1.05 and 1.15 at low-power operation (1 W) and high-power operation (3 W), respectively. Figure 4 shows the three-dimensional (3D) beam profile and the Gaussian fit of the beam at high-power operation.

The efficiency of heat dissipation can be characterized by measuring the lasing wavelength shift with pump power.¹ The lasing wavelength is measured by optical spectrum analyzer. The measured lasing wavelength shift of our VECSEL is $0.22 \text{ nm/kWcm}^{-2}$. This slow lasing wavelength shift reflects efficient heat dissipation at the indium-solder-CVD diamond interface.

The ultrashort Er/Yb-codoped single-mode fiber lasers are very attractive to achieve compact high-power single-longitudinal-mode lasing. Two pump schemes are usually used for fiber lasers: Multimode cladding-pumping and single-mode core-pumping schemes. The core-pumping scheme leads to significantly improved pump absorption and pump efficiency compared to the cladding-pumping schemes.⁸ Especially for an ultrashort single-mode fiber laser, a high-power VECSEL with a diffraction-limited circular beam can be an efficient pump source since it is efficiently coupled into the single-mode core by an objective lens. We used a VECSEL operating at 976 nm to pump the core of an ultrashort highly Er/Yb-codoped single-mode phosphate fiber laser. The fiber length is only 3 cm, and bare fiber is installed in a low index glass tube having an inner hole diameter of $135 \mu\text{m}$ without any cooling. This single-mode phosphate fiber has a core diameter of $13 \mu\text{m}$ and supports the fundamental mode at 1535 nm.^{9,10} Since the phosphate glass has high solubility of rare-earth ions and low clustering effects, the core is highly doped with $1.1 \times 10^{26} \text{ ions/m}^3$ of Er^{+3} and $8.6 \times 10^{26} \text{ ions/m}^3$ of Yb^{+3} to optimize pump absorption and energy transfer from Yb^{+3} to Er^{+3} and to achieve high gain. Two dielectric coating mirrors are used to form the laser cavity. On the pump side, the mirror, which is directly coated on the one end of the phosphate fiber, has the reflectivity of $R_1(\lambda_s=1535 \text{ nm}) > 98\%$ at the signal wavelength and $R_1(\lambda_p=976 \text{ nm}) < 5\%$ at the pump wavelength. The output mirror has a high reflectivity of $R_2(\lambda_p) > 96\%$ at the pump wavelength and $R_2(\lambda_s)=30\%$ at the signal wavelength. A simple and efficient pumping is achieved by directly coupling the circular beam of the VECSEL into the single-mode core of the fiber using a conventional objective lens. Figure 5 shows the single-mode fiber laser output

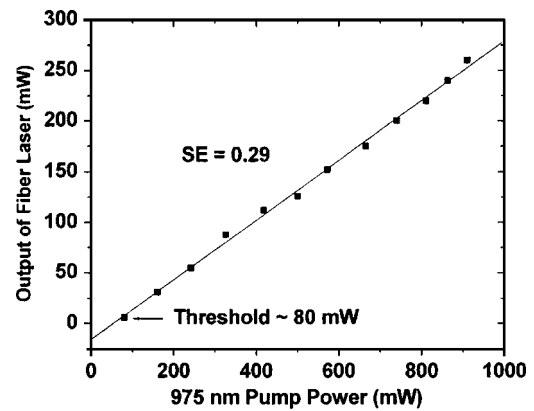


FIG. 5. Single-mode fiber cw output power at 1535 nm vs the VECSEL launching power at 976 nm.

power as a function of VECSEL pump power. A threshold of 80 mW and SE of 29% relative to the launched pump power is achieved. An output power in excess of 250 mW at 1535 nm is obtained without any cooling.

In comparison with the above cladding-pumping single-mode fiber lasers that are built by the same kind of fiber and similar cavity, with the slope efficiency of 10% and 20% at low pump power for 3 cm long and 7.1 cm long fiber,¹⁰ respectively, a significant improvement in the SE is achieved by using the VECSEL core pumping.

In conclusion, we developed and demonstrated a high-brightness and high-power VECSEL. Over 3 W TEM₀₀ output power and high slope efficiency (0.44) has been achieved at room temperature. Good surface quality and thermal management is the key for the VECSEL performance. The laser acts as an excellent pump source for the single-mode-fiber laser. An output power in excess of 250 mW at 1535 nm with a SE of 29% from a 3 cm long single-mode-fiber laser was obtained without any cooling. Simple and efficient VECSEL pumping of the fiber laser should allow the development of even shorter, more compact, fiber lasers and arrays.

The authors would like to thank Li Li, Elena Temyanko, Robert Bedford, and Marc Schillgalies for their technical support. This work is supported by the Air Force Office of Scientific Research through a MRI Program F49620-02-1-0380.

¹M. Kuznetsov, F. Hakimi, R. Sprague, and A. Mooradian, *IEEE J. Sel. Top. Quantum Electron.* **5**, 561 (1999).

²S. Lutgen, T. Albrecht, P. Brick, W. Reill, J. Luft, and W. Spath, *Appl. Phys. Lett.* **82**, 3620 (2003).

³J. Chilla, S. Butterworth, A. Zeitschel, J. Charles, A. Caprara, M. Reed, and L. Spinelli, *Proc. SPIE* **5332**, 151 (2004).

⁴A. C. Tropper, H. D. Foreman, A. Garnache, K. G. Wilcox, and S. H. Hoogland, *J. Phys. D* **37**, R75 (2004).

⁵C. Stewen, K. Contag, M. Larionov, A. Giesen, and H. Hügel, *IEEE J. Sel. Top. Quantum Electron.* **6**, 650 (2000).

⁶J. Hader, J. V. Moloney, S. W. Koch, and W. W. Chow, *IEEE J. Sel. Top. Quantum Electron.* **9**, 688 (2003).

⁷A. R. Zakharian, J. Hader, J. V. Moloney, S. W. Koch, P. Brick, and S. Lutgen, *Appl. Phys. Lett.* **83**, 1313 (2003).

⁸D. Kouznetsov and J. V. Moloney, *J. Opt. Soc. Am. B* **19**, 1259 (2002)

⁹P. Leproux, S. Février, V. Doya, P. Roy, and D. Pagnoux, *Opt. Fiber Technol.* **6**, 324 (2001).

¹⁰T. Qiu, L. Li, A. Schulzgen, V. L. Temyanko, T. Luo, S. Jiang, A. Mafi, J. V. Moloney, and N. Peyghambarian, *IEEE Photonics Technol. Lett.* **16**, 2592 (2004).